Physica E 42 (2010) 2618–2621

Contents lists available at ScienceDirect

Physica E

journal homepage: www.elsevier.com/locate/physe

Efficient injection-type ballistic rectification in Si/SiGe cross junctions

D. Salloch [a,*], U. Wieser [a], U. Kunze [a], T. Hackbarth [b]

[a] Werkstoffe und Nanoelektronik, Ruhr-Universität Bochum, D-44780 Bochum, Germany
[b] DaimlerChrysler Forschungszentrum Ulm, Wilhelm-Runge-Straße 11, D-89081 Ulm, Germany

ARTICLE INFO

Article history:
Received 28 August 2009
Accepted 24 March 2010
Available online 30 March 2010

Keywords:
Ballistic transport
Si/SiGe heterostructures
Ballistic rectification
Quantum wires

ABSTRACT

Tunable inertial-ballistic rectification is studied in a nanoscale injection-type Si/SiGe rectifier in the hot-electron regime. The rectifier consists of a cascade of two nanoscale cross junctions in series. Two pairs of opposing current injectors merge under 30° into a straight central voltage stem. The electron densities in the injectors and the stem can be adjusted separately by two local top-gates. The measurements reveal a substantial efficiency increase for a nearly depleted stem. The efficiency of ballistic rectifiers can be expressed by the transfer resistance R_T (output voltage divided by input current), the best value we achieve is 800 Ω.

1. Introduction

In the diffusive transport regime, which is relevant for conventional semiconductor devices, electrons are accelerated by an electric field between a large number of individual scattering events. In this case the average transport velocity is given by the electron drift velocity v_D. If the relevant device dimensions are reduced below the electron mean free path the system changes into the ballistic regime which is dominated by elastic scattering of electrons at the device boundaries. In this regime the momentum of the electrons plays a decisive role and the device properties directly depend on the device geometry. A ballistic rectifier differs in two major points from conventional rectifiers like *pn* junctions and Schottky contacts. Firstly, an ideal ballistic rectifier is free from any potential barriers and a zero cut-in voltage is expected for the onset of rectification. Secondly, the rectification efficiency depends on the detailed device geometry and the electron velocity. Ballistic full-wave rectification has been realized in nanoscale three-terminal Y- [1–3] and T-branch junctions [4,5] as well as four-terminal reflection- [6,7] or injection-type [8] cross junctions in the non-linear response regime. The rectified signal of three-terminal devices arises either solely (T-branch) or in addition to an inertial-ballistic component (Y-branch) from a mode-controlled contribution, which relies on the different number of current-carrying modes in the opposed injector branches. Also four-terminal junctions can be partly [6,7] or, in a bridge-type geometry [9,10], completely determined by mode-controlled mechanisms. Suitable four-terminal ballistic rectifiers enable to separate the inertial-ballistic from the mode-controlled signal. The rectifiers consist of a straight central voltage stem and two opposing current injectors which merge under an injection angle ϕ into the central stem [8]. The inertial-ballistic rectified signal develops between the upper and lower end of the central stem upon injecting a current between the injector branches.

In this paper, we investigate the influence of a locally modulated electrochemical potential in the stem region on the transfer resistance R_T (output voltage divided by input current) for a cascade of two inertial-ballistic four-terminal rectifiers in series. The potential modulation is obtained by two nanoscale top-gates. Furthermore, the influence of the injector pairs among each other in individual operation is investigated.

2. Sample preparation

The rectifier is fabricated from a high-mobility $Si/Si_{0.7}Ge_{0.3}$ heterostructure. The layer sequence consists of a relaxed graded SiGe buffer layer, a pseudomorphically strained 8-nm-thick Si quantum well containing the two-dimensional electron gas (2DEG), a 14-nm-thick intrinsic $Si_{0.7}Ge_{0.3}$ spacer and a 10-nm-thick Sb-doped *n*-$Si_{0.7}Ge_{0.3}$ supply layer. The heterostructure is covered by a 6-nm-thick Si cap layer. The 2DEG is located only 30 nm below the sample surface that allows the creation of a strong confinement potential by shallow etching of the lateral layout and good top-gate control of the electron density. However, a positive top-gate voltage is necessary to accumulate electrons in the current leads and the voltage stem. The electron density and mobility in the strained Si channel are extracted from Shubnikov–de Haas (SdH) oscillations measured on a conventional Hall-bar structure with a top-gate voltage of $V_G = 150$ mV at $T = 1.5$ K. The mobility amounts to

* Corresponding author.
E-mail address: daniel.salloch@rub.de (D. Salloch).

1386-9477/$ - see front matter © 2010 Elsevier B.V. All rights reserved.
doi:10.1016/j.physe.2010.03.021

$1.25 \times 10^5\,\mathrm{cm^2\,(Vs)^{-1}}$ at an electron density of $2.3 \times 10^{11}\,\mathrm{cm^{-2}}$. Considering a twofold valley degeneracy we calculate a 2D elastic mean free path of about 0.7 μm.

The fabrication process starts with the preparation of alignment marks defined by conventional UV lithography and plasma etching. Subsequently, ohmic contacts are prepared by implantation of phosphorus ions with an energy of 30 keV and a dose of $2 \times 10^{15}\,\mathrm{cm^{-2}}$. Recrystallization of the amorphous surface layer and donor activation are achieved by annealing the sample at 560 °C for 30 min in nitrogen atmosphere. A mix-and-match process which combines high-resolution e-beam lithography and standard UV lithography defines the lateral layout of the nanoscale rectifier, a second set of local alignment marks for the top-gates and the large-area leads and contacts of the device. For high-resolution e-beam lithography we use calixarene as a negative-resist. Leads and contacts are prepared in a standard photoresist, which is spin coated, exposed and developed after e-beam lithography [11]. The combined resist pattern is transferred into the heterostructure using a low-damage inductively coupled plasma (ICP) process with an ICP power of 400 W and an additional bias power of 40 W. The process gases are CF_4 and O_2 with a flow rate of 11 and 1 sccm, respectively. The small bias voltage ensures low plasma ion energies, with a dominant chemical component of the etch process. We achieve an etch depth of 50 nm during 20 s for the given heterostructure. After patterning, the metallic contacts are prepared by evaporating 25 nm Ti and 100 nm Au on top of the implanted areas. Contact properties are improved by sintering the sample at 400 °C for 60 s. Finally, two local Schottky top-gate electrodes are defined by e-beam lithography (positive resist PMMA), metallisation of 10 nm Ni and 25 nm Au and lift-off. The position of the local top-gates is adjusted using both sets of alignment marks which gives a position accuracy of about 20 nm with respect to the device structure. The leads and contacts for the top-gates are defined by UV lithography and a lift-off process.

The layout of the device is shown in Fig. 1(a) before and (b) after deposition of the top-gates. The cascaded rectifier is composed of a common central voltage stem between two voltage probes U and L and two pairs of current injecting branches (1, 2) and (3, 4). The stem has a length of 2 μm and a width of 490 nm while the width of the injectors amounts to 220 nm. The angle between current injectors and voltage stem is $\phi = 30°$ and the distance between the junctions is 700 nm. The electron density is adjusted by means of the top-gate voltages. The gate SG covering the whole stem controls the electron density in the stem region whereas the gate IG allows to modify the conductance of the injectors.

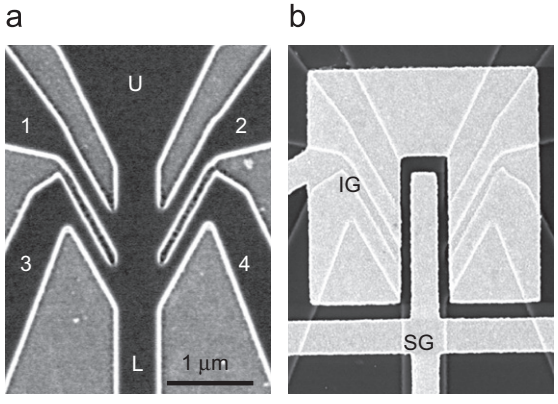

Fig. 1. Scanning electron micrograph of the ballistic rectifier (a) before and (b) after split gate deposition with current leads (1–4), upper (U) and lower (L) voltage probe, injector gate (IG) and stem gate (SG).

3. Results and discussion

The electronic characterisation is performed at $T = 4.2$ K. Using lock-in technique the dependence of the differential conductance on the gate voltages are measured at a modulation frequency of 433.3 Hz and a modulation voltage of 100 μV rms. Fig. 2(a) shows the differential conductance of the injector pairs for a fixed stem-gate voltage $V_{SG} = 100$ mV and varying V_{IG}. The threshold voltage is $V_{th,IG} = -0.04$ V and the maximum conductance including series resistances from contacts and leads reaches up to 125 μS for injector pair (1, 2). For the device operation the injectors need to be conducting well to ensure an efficient injection of electrons into the stem and a low input resistance of the device. In Fig. 2(b) the injector-gate voltage is fixed to $V_{IG} = 300$ mV and the differential conductance is recorded as a function of the stem-gate voltage V_{SG}. The threshold voltage of the stem is $V_{th,UL} = -0.09$ V and thus higher than the threshold voltage of the injectors which is -0.18 V. This ensures that the injectors are conducting well, even if the stem is pinched off.

For DC measurements of the non-linear input characteristics and the transfer characteristics, we use a Semiconductor Parameter Analyser and drive the input current through the injectors by applying a voltage in push-pull fashion, i.e. $V_1 = -V_2$ ($V_3 = -V_4$). Fig. 3 shows the *I–V* characteristics of the injectors for fixed $V_{IG} = 300$ mV and V_{SG} as parameter. Both characteristics (a) and (b) show linear behaviour for $|V_{12}| < 30$ and $|V_{34}| < 30$ mV, respectively. For higher input voltages the curves are non-linear, which is attributed to carrier heating, a voltage depending number of current-carrying transport modes inside the injectors and voltage dependent contact resistances. The influence of the stem-gate voltage is relatively weak. This is due to the fact that only the broader regions in the cross junctions of the stem are covered by the stem gate. Both injector pairs nearly show the same behaviour. The transfer characteristics are measured as difference voltage $V_{UL} = V_U - V_L$, which represents the inertial-ballistic rectified signal, as a function of the injector current [12]. In Fig. 4(a, b) the transfer characteristics of injector pair (1, 2) and (3, 4) are shown for fixed $V_{IG} = 300$ mV and different V_{SG}. For both injector pairs the rectified signal starts roughly parabolic followed by a linear characteristic whose slope is widely controlled by the stem gate voltage. Unexpectedly, the characteristics are nearly an ideal V-shape in contrast to earlier experiments where the rectified signal always depends parabolic on the input current. The slope of the transfer characteristics decreases with increasing stem gate voltage and, hence, the output signal is highest for stem

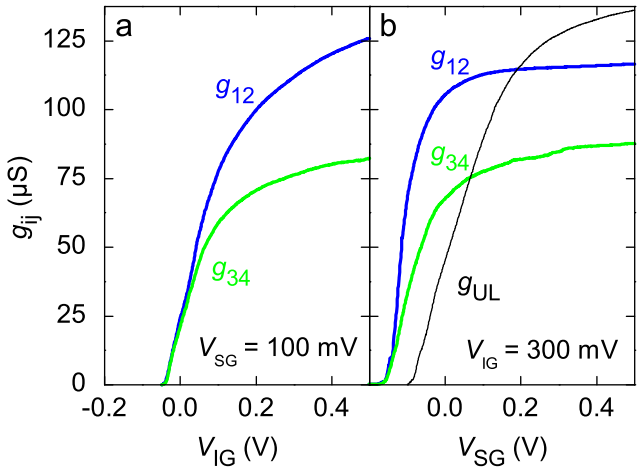

Fig. 2. Differential conductance g_{ij} between leads *i* and *j* vs (a) V_{IG} and (b) V_{SG} for constant $V_{SG} = 100$ mV, $V_{IG} = 300$ mV, respectively.